19

Tissue visualization mediated by nanoparticles: from tissue staining to mass spectrometry tissue profiling and imaging

Lenka Kolářová[1#], Petr Vaňhara[2#], Eladia María Peña-Méndez[3], Aleš Hampl[2,4] and Josef Havel[1,2,5,6*]

[1]Department of Chemistry, Faculty of Science, Masaryk University, Kamenice 5/A14, 625 00 Brno, Czech Republic
[2]Department of Histology and Embryology, Faculty of Medicine, Masaryk University, Kamenice 3/A1, 625 00 Brno, Czech Republic
[3]Department of Analytical Chemistry, Nutrition and Food Science, Faculty of Chemistry, University of La Laguna, Campus de Anchieta, 38071 La Laguna, Tenerife, Spain
[4]International Clinical Research Center, St. Anne´s University Hospital, Brno, Czech Republic, Pekařská 53, 656 91 Brno, Czech Republic
[5]Department of Physical Electronics, Faculty of Science, Masaryk University, Kotlářská 2, 611 37 Brno, Czech Republic
[6]R&D Centre for Low-Cost Plasma and Nanotechnology Surface Modifications, CEPLANT, Masaryk University, Kotlářská 2, 611 37 Brno, Czech Republic
[#]These authors contributed equally.

Outline:

Introduction

For decades, visualization of cell and tissue structures by chemical staining developed for optical microscopy was the only option for a clinical histopathological diagnosis or biomedical research in a tissue context. A cardinal breakthrough was later achieved by the introduction of antibody-based techniques that provided spatial resolution and antigen specificity at the cellular and sub-cellular levels. Presently, classical methods of tissue analysis are complemented with various instrumental methods to provide global information on tissue architecture, reflecting the chemical composition of the tissue, including spatial distribution of metabolites, regional structural differences of the extracellular matrix or secreted proteins and other large molecules. These techniques include Raman spectroscopy (RS), magnetic resonance imaging (MRI), ultrasonography (US), computed tomography (CT) or positron emission tomography (PET), single-photon emission CT (SPECT) or mass spectrometry (MS). In this review, we provide a brief overview of the application of nanotechnology in histology methods, particularly in bioanalytical tissue MS imaging.

From tissue staining to tissue imaging

Tissue staining is an established histological technique that reveals structural patterns that are not clear or sufficiently visible to be observed directly. The first dyes used for staining of tissue structures were colored substances isolated from natural resources—e.g., indigo, saffron, hematoxylin, azocarmine, and orcein. These dyes were commonly used for dyeing textile fibers and later found wide application in histology. The onset of synthetic dyes further enhanced histopathological analyses since the invention and application of aniline dyes in 1856 [1]. However, various tissues, including neural or lymphatic tissue, resisted staining using large molecular dyes. When the impregnation by silver salts and other non-classical-dyes was introduced to histological analysis [2], fine molecular structures of complex organs were revealed—e.g., reticulin networks in the spleen or the architecture of the brain isocortex (Fig. 19.1A). Decades later, the application of fluorescent dyes or enzymes linked to specific antibodies, together with confocal microscopy, shifted histological analysis from subjective morphological evaluation to the analysis of particular molecular patterns or epitopes even in an automated manner [3]. Advances in analytical chemistry, particularly in MS, and its orientation in complex biological problems, contributed to the development of techniques for the direct analysis of chemical tissue composition, thereby enhancing the potential of current diagnostics in cancer [4] or pharmaceutical research [5]. Mass spectra with individual peaks corresponding to molecules of a particular molecular weight and charge (i.e., the m/z ratio) provide individual tissues with their unique spectral fingerprint (Fig. 19.1B) and an input for "bottom-up" proteomics. The progress of micromanipulation techniques, such as laser-captured microdissection allowed topologically highly correlated MS-based proteomic analysis on very small but precisely defined cell populations [6].
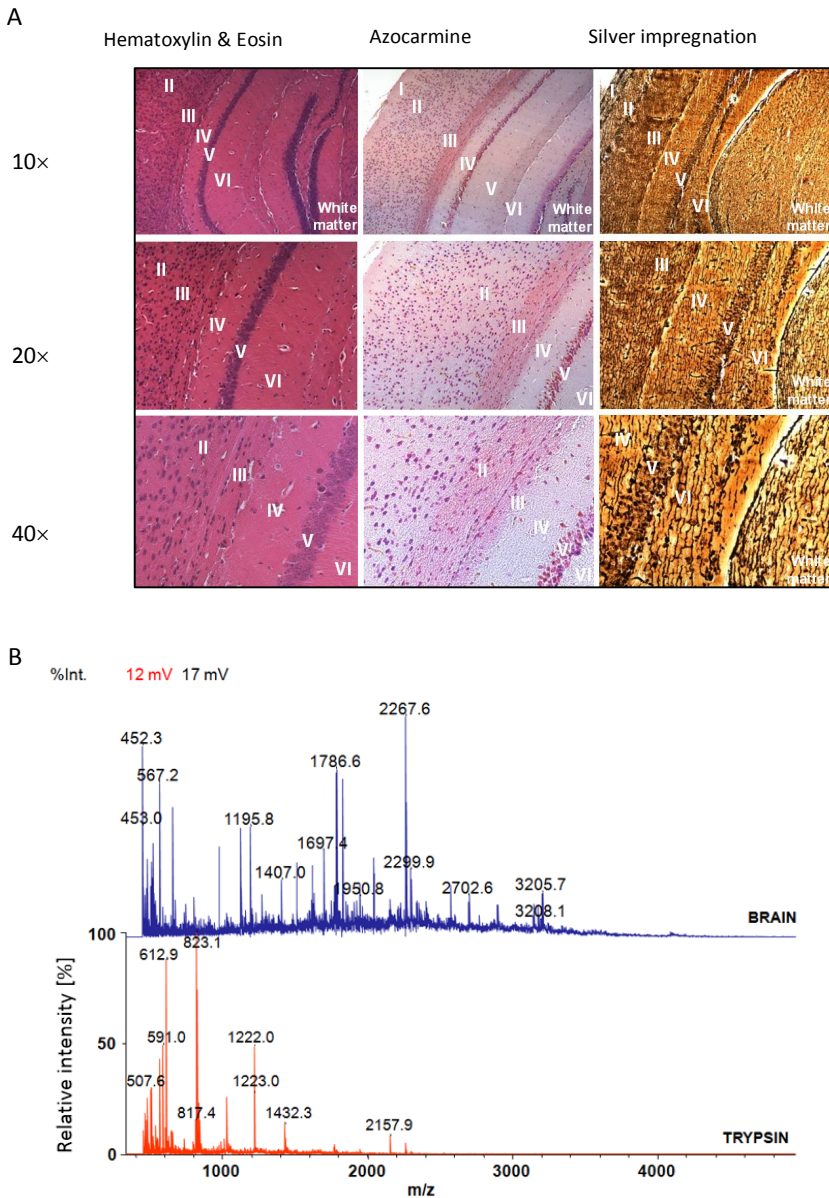
FIGURE 19.1

(A) Architecture of the mouse isocortex and adjacent cerebral white matter, visualized by classical histological techniques. Brain tissue was fixed in formalin and embedded in paraffin (FFPE). Sections of the isocortex were stained with hematoxylin and eosin, azocarmine and silver impregnation according to standard protocols [7]. Roman numerals correspond to individual layers in the isocortex (I: *Lamina zonalis*; II: *L. granulairs externa*; III: *L. pyramidalis*; IV: *L. granularis interna*; V: *L. ganglionaris*; VI: *L. multiformis*). Deposition of silver nanocrystals within neural structures and neurons reveals structural patterns that are poorly distinguished by standard staining. (B) A unique molecular fingerprint of mouse brain tissue. The spectral profile of the digested surface proteins was generated by matrix-assisted laser desorption/ionization-time-of-flight (MALDI TOF) MS (blue). Brain tissue in the form of FFPE sections was deparaffinized and trypsinized (red) prior to MS

Presently, the term "tissue imaging" is dedicated to advanced methods of visualizing tissue structures ranging from *in vivo* imaging of whole organs to high-resolution cell tracking or revealing the chemical composition and metabolomic profiles. For decades, classical histological methods have been based on specific chemical staining of tissue sections, selective for proteins, peptides, lipids, metabolites or other biomolecules or drugs. Despite precise positional information within a tissue, standard topological dyes have provided only limited information concerning chemical composition or structural specificity. However, antibody-based techniques developed for visualization of fixed structures are generally not compatible with imaging *in vivo* due to protein degradation or limited penetration into tissues. Nanoparticles containing a metallic core and a functionalized shell that were recently introduced to bioimaging technology showed surprisingly effective capability to migrate to the desired site, interact with the target tissue and deposit in specific sites.

Nanoparticles as visualization agents

A nanoparticle (NP) is defined as a single unit with a size varying between ~1 and 100 nm and showing uniform parameters and properties that are not present on a larger scale [8]. Recent advances in nanotechnology brought NPs to the broad interest of the scientific community due to their unique chemical, optical, electronic, magnetic and structural properties. NPs have found wide applications in biomedicine, ranging from research to diagnostics, prediction or therapeutics [9]. Because the size of NPs reaches cellular or sub-cellular levels while maintaining their capability to directly interact with molecular structures, NPs are greatly attractive in fluorescent microscopy as quantum dots [10, 11] or contrasting agents for tissue *in vivo* imaging (MRI), particularly regarding the labeling and tracking of migrating cancer or stem cells [12] or enhancing other types of analysis—e.g., MS. NPs can be synthesized from various materials ranging from carbon to metals and functionalized according to the desired function or visualization techniques. Functionalization of NPs covers a broad range of modifications of the NP core or engineering of an NP shell. Properties of NPs can be further tuned to a particular task by the composition of different biocompatible compounds that allow use in living cells. This is particularly true for many cancers that preferentially uptake various metabolites or biomolecules compared with normal tissue. Iron oxide NPs coated with the heavy chain of human ferritin (M-HFn) were found to interact with the transferrin receptor that is predominantly expressed on cancer cells. The iron core possesses catalytic activity and allows the oxidation of standard peroxidase substrates— e.g., tetramethylbenzidine or diazoaminobenzene. The deposition of M-HFn NPs in cultured cancer cells or within a fixed tissue allowed for precise identification of malignant cells in histological sections [13]. Recently, fluorescent nanodiamonds were applied to track implanted lung progenitor cells during engraftment from intravenous administration to final homing into terminal bronchioles [14]. Therefore, simple administration of such biospecific NPs provides an analytical output without any further targeting ligand of contrasting substrate. Specific interaction of engineered NPs with cellular or tissue structures opens a possibility to detect bound para- or supermagnetic NPs *in vivo*—e.g., using MRI or other multimodal imaging techniques such as CT, SPECT or fluorescence-based techniques. In a breast cancer cell line study, Tietz and colleagues encapsulated an iron oxide core in an epichlorohydrin cross-linked dextran polymer, conjugated with a cyclopentapeptide with high affinity to a CXCR4 chemokine receptor. Breast cancer MDA-MB-231 cells overexpressing CXCR4 preferentially bound CXCR4-specific NPs and provided a negative contrast MRI image [15]. Iron oxide NPs were used for MRI tracking of implanted mouse embryonic stem cells into the site of the lesion where the labeled cells provide a hypointense MRI signal [16]. The superparamagnetic iron oxide NPs are generally safe and well-tolerated compounds [17] currently approved for administration in patients using various modalities.

Lanthanide core NPs specifically influence the relaxation times of protons in their close proximity and, compared with iron oxide NPs, provide a positive MRI contrast. Contrasting agents based on gadolinium (Gd^{3+}) chelates, however, may induce adverse reaction in some patients—e.g., nephrogenic systemic fibrosis [18]. To overcome this obstacle, modification of the structures coating the Gd core has been described—e.g., polyethylenglycol/polyethylenimine [19], silica coating [20], various metal-organic frameworks (MOFs) [21] or nanocarbon (nanodiamonds) [22]. Due to their molecular structure, MOFs are highly attractive as drug-delivery vehicles or imaging agents (Fig. 19.2). Targeted complex Gd NPs then show high specificity to the investigated tissue—e.g., cancer-lesioned liver [23] or melanin-containing melanoma cells [24]. Replacement of the coated core metal with an inert element—e.g., gold—and building up a scaffold with similar structural properties to the extracellular matrix or a cell membrane have decreased the toxicity of MRI-contrasting NPs, enhanced the imaging properties [25] and also allowed for multiple analysis using, for example, fluorescence sorting, MS profiling, antibody-based techniques, magnetic labeling or electron microscopy [22, 26, 27]. The mesoporous silica-coated hollow manganese oxide demonstrated low cellular and systemic toxicity when electroporated into the mesenchymal stem cells (MSCs) and tracked by MRI after stereotactic injection into the putamen of the mouse. Moreover, MSCs containing silica-coated manganese NPs retained their viability, and their differentiation potential was uncompromised. Importantly, the architecture of mesoporous silica shell NPs provided access of water molecules to the manganese core and enhanced the positive contrast of the MR image. Deposition of labeled MSCs in hyperintense MRI loci allowed stable tracking with high spatial resolution over prolonged time periods [28].

Recently, nanoscale metal-organic frameworks (NMOFs) emerged as promising biomedical or bioengineering tools for imaging and drug delivery [29-31]. NMOFs are a new class of hybrid materials in nanometer size consisting of metal ions and organic bridging ligands (Fig. 19.2). The chemical properties of these materials, such as their structural and molecular diversity, type of metallic core (e.g., Yb, Gd, Mn, or Fe), high loading capacity, and intrinsic biodegradability make them suitable for direct *in vivo* imaging using near-infrared microscopy [32] or MRI [33].
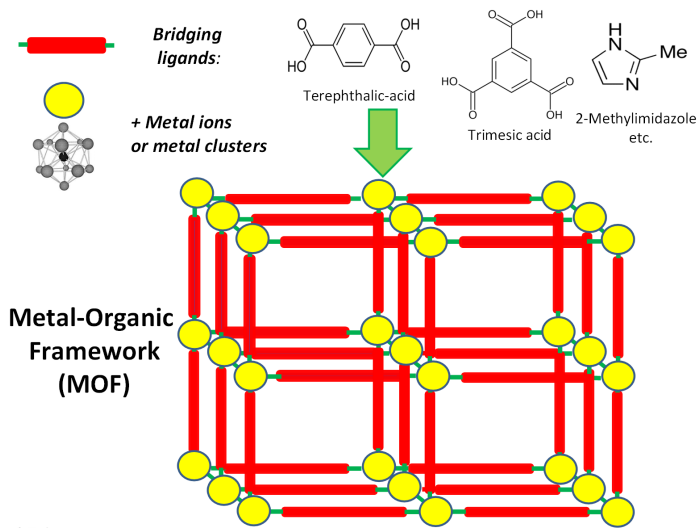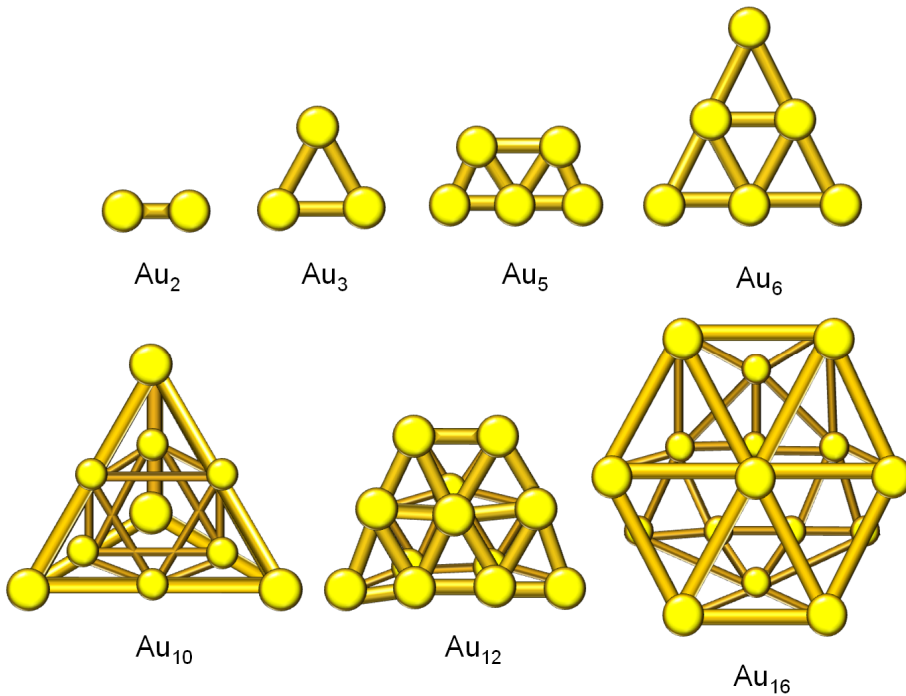

FIGURE 19.2
Molecular structure of an MOF NP

Gold NPs (AuNPs) are a promising class of NPs with a lower frequency of adverse effects of lanthanide NPs in vivo and a longer life-time than iron NPs. Individual AuNPs (Fig. 19.3) or their clusters (Fig. 19.4) can be directly modified by various structures that either improve a detection method, enhance specificity or reduce toxicity and improve clearance. For example, nanoflares are highly functionalized NPs that bring extreme detection specificity to the level of single molecules of nucleic acids. Thus, the conjugation of specific oligonucleotides to AuNPs combines very high specificity with a potent fluorescence activity and low toxicity to the cell. Standard techniques for mRNA detection are based on the detection of an interaction event between a fluorophore-labeled oligonucleotide with its target sequence. However, major obstacles lie in the delivery method into cells, a high background compromising the specificity of the assay and enzymatic degradation of the reporters. AuNP-based nanoflares possess the unique capability of detecting individual mRNAs in living cells without enzymatic degradation of the vehicles or the need for transfection reagents for delivery [34, 35].
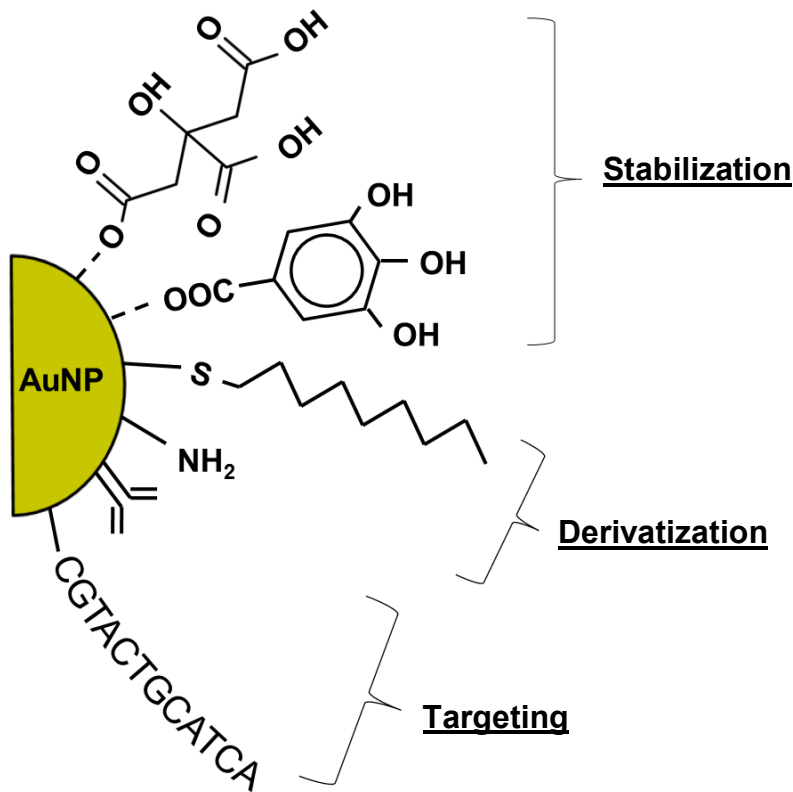
FIGURE 19.3
Example of direct modifications of AuNPs. AuNPs can be stabilized using citric acid or gallic acid. Derivatization by introducing various functional groups or even biomolecules (e.g., thiol, amino, antibody, and oligonucleotides) can enhance the binding specificity to particular tissue structures, antigens or even individual sequences of DNA or RNA. Dashed or full lines indicate non-covalent or covalent bonds, respectively

FIGURE 19.4

AuNPs form clusters of various sizes and complexity. Gold clusters up to Au_{10} are known to be planar, higher Au clusters possess three-dimensional structure, and some of them (Au_m, where m=16,17,18) might be empty, representing gold fullerenes, which are hollow gold cages that can form endohedral complexes—e.g., M@Au_{16}, where M is a foreign metal inside the cage

Therefore, NP engineering defines physical parameters that are critical for the particular imaging method but also determines biological properties, such as target specificity, migration through the tissue environment, retention in the vascular system, renal excretion or the efficacy of the cellular uptake, which can dramatically influence the information value of the diagnostic or analytical output (Fig. 19.5).
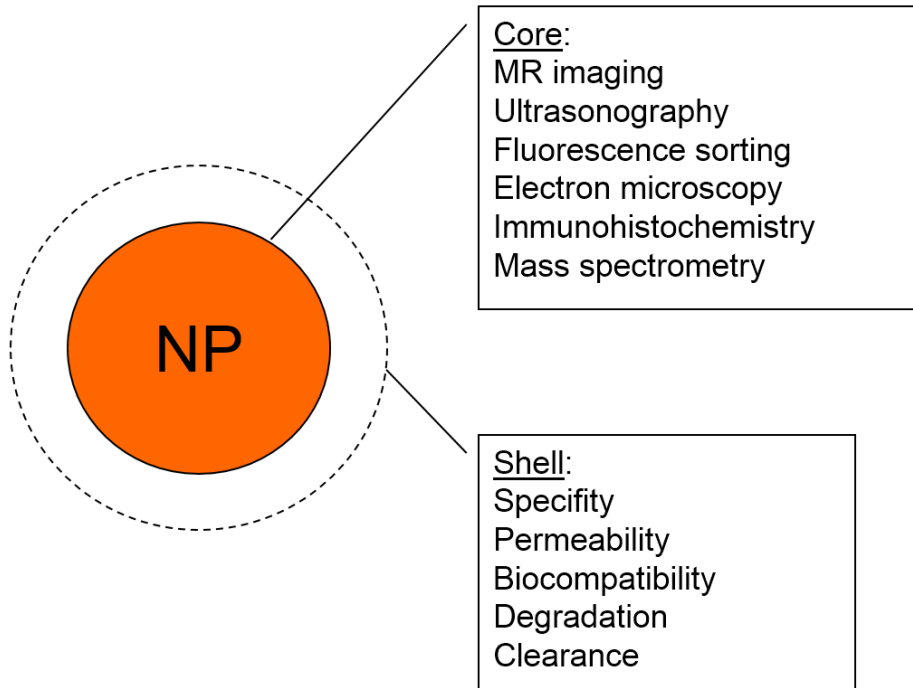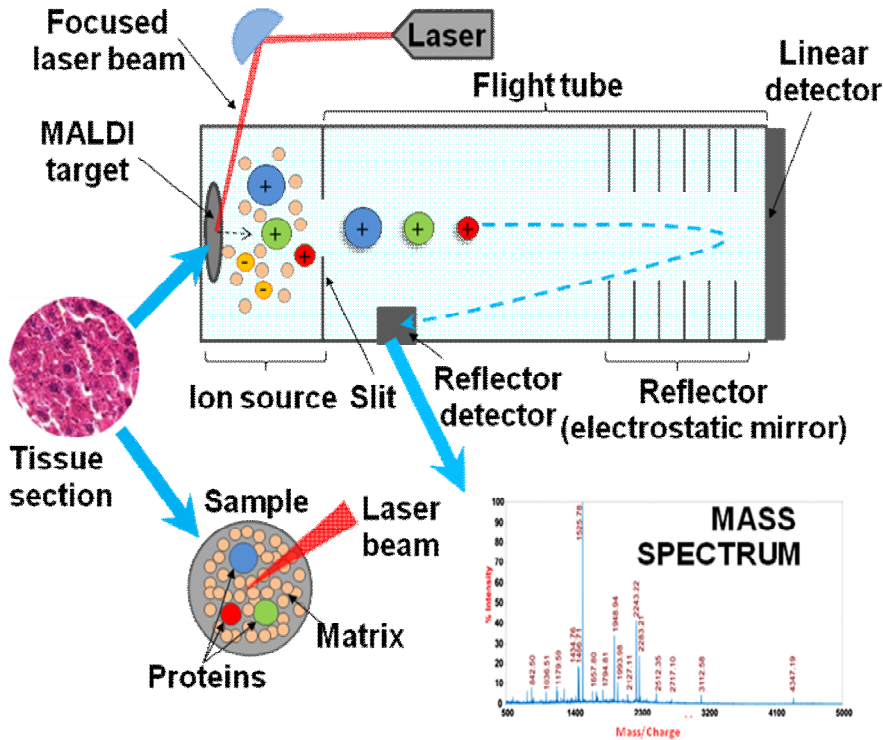
FIGURE 19.5

Engineering of the core and shell determines performance in various imaging techniques and targeting specificity, and prevents degradation or adverse effects *in vivo*

Tissue imaging by MS

MS allows the rapid detection, localization and identification of many molecules from the very simple to the most complex (e.g., biomolecules). Tissue MS is a label-free technique that can provide detailed understanding of biological processes in a broad cellular context and whole biological systems. A principle of MS techniques is demonstrated in the MALDI-TOF MS example summarized in Fig. 19.6. The development of imaging MS (IMS) provided the unique ability to analyze hundreds of analytes in a one experiment without prior knowledge of the tissue composition or the use of antibodies or staining reagents. Another advantage of this technique is the maintenance of spatial molecular patterns because tissue samples are analyzed without prior homogenization (mechanical disruption of tissue, creating a homogenous mixture) or fractionation (division of homogeneous mixture into individual fractions) [36, 37]. Homogenization and fractionation belong to classical approaches of sample preparation; however, these techniques affect the distribution of particular molecules (spatial information) and destroy morphological structures. Moreover, the IMS approach can visualize the global biochemical heterogeneity of individual cell populations and tissue structures at the single-cell level [38]. IMS can be applied in a wide area of "omics" research such as proteomics, lipidomics,

metabolomics, metallomics, and drug discovery, and is a topic that was reviewed in detail recently [39].

FIGURE 19.6

Principle of MALDI-TOF MS. Tissue molecules co-crystallized with a matrix (defined below) are desorbed by a laser beam from a sample surface. Ions enter into the flight tube towards a detector. The time of flight and intensity of the signal are recorded; next the ratio of the molecular weight (m/z) to charge is determined

Depending on the experimental design, the output is either a single mass profile of a nonspecific tissue region or a homogeneous cell population, or a panel of mass spectra recorded in high resolution from defined coordinates and containing spatial information [40]. The IMS approach efficiently combines the analysis of molecular species and their distribution together with morphological and histopathological information. Moreover, fixed tissues prepared for routine histology are compatible with IMS or other various modifications of MS, enabling analysis of various samples stored at medical facilities [41]. However, IMS requires modifications of virtually all steps of the standard "profiling" MS protocol. To achieve a desired resolution, the sample preparation and application retrieving the surface molecules for ionization, instrumental setup, data acquisition and mass spectra analysis in parallel with histological assessment need to be optimized [42-45]. A scheme depicting the difference between MS profiling and MS imaging is shown in Fig. 19.7.
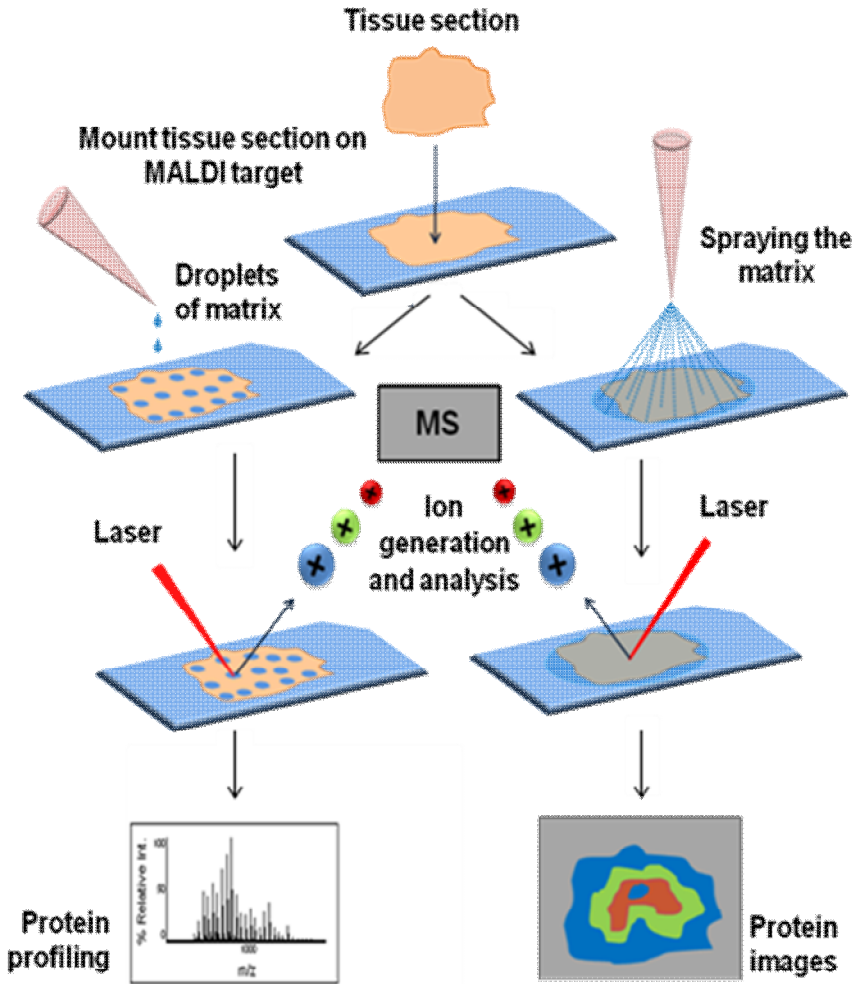
FIGURE 19.6
Principle of mass spectrometry profiling and imaging on intact tissue sections

Ionization methods for IMS

Ionization is a critical step in the entire process of IMS, determining the quality of recorded spectra, spatial resolution and content of biologically relevant information. Presently, there is a broad range of surface ionization methods adopted for IMS from bioanalytical MS; however, MALDI MS, secondary ion MS (SIMS) and desorption electrospray ionization (DESI) are the most common.

MALDI MS

MALDI is a soft ionization technique based on mixing a sample with an excessive amount of a matrix and subsequent desorption and ionization of the sample molecules by a short (~ns) laser pulse usually

in a high vacuum (about 10^{-4} Pa) [46]. The matrix plays a key role in the absorption of laser energy of a certain wavelength, which is then passed to the analyte, causing a transition of the analyte from the solid phase into the gas phase and preventing fragmentation molecules of the sample by using a direct laser beam. The matrix is at the same time a donor or acceptor of protons to the sample molecules in the positive or negative mode. The mechanism of proton transfer from the matrix to the analyte remains unclear. This technique preferentially provides pseudomolecular $[M \pm H]^{\pm}$ ions of the analyte but sometimes can be observed in the spectra of other ions, such as $[M + 2H]^{2+}$, $[M + 3H]^{3+}$ ions or dimers $[2M + H]^{+}$, and others. MALDI enables the ionization of biomolecules over a wide mass range, including DNA, peptides, proteins, lipids and many other substances. MALDI MS is often the chosen bioanalytical method because of its sensitivity, its tolerance to impurities and simple preparation of the sample [38].

The correct choice of matrix is one of the most important steps in MALDI IMS. As the matrix, organic aromatic acids are usually used. Each matrix is suitable for different analytes. For example, the most commonly used matrix in MALDI-TOF of cellular or tissue samples is sinapinic acid suitable for the detection of higher molecular weight proteins, α-cyano-4-hydroxycinnamic acid for the detection of lipids and lower molecular weight peptides and 2,5-dihydrobenzoic acid or 2,6-dihydroxyacetophenone for the ionization of phospholipids and drugs [47]. Various matrices differently affect desorption and, thus, ionization of the analyte. The interaction of the analyte with the matrix might also improve the ionization efficiency. The application of a MALDI matrix on the sample of tissue section affects substantially the assay output. In MALDI IMS of a tissue section, the matrix solution needs to be homogeneously deposited over the sample—e.g., by spraying the matrix over the entire surface of the tissue. However, the regions desired for single profiling can be defined by simple deposition of matrix droplets to particular regions of the tissue section [48].

Manual methods of matrix deposition such as airbrush spraying or dipping the tissue sections into a matrix-containing solution usually suffer from poor reproducibility [49]. Automated deposition allows the deployment of a very thin layer of matrix with an IMS quality suitable also for high-throughput preparations [50]. The most common mass analyzer in combination with the MALDI technique is the TOF, which provides high mass resolution, excellent mass accuracy, and a rapid acquisition rate over a large mass range [51].

SIMS

SIMS was the first ionization technique in MS used for chemical imaging [52]. The main advantage of SIMS is the spatial resolution level at the submicron level as low as 50 nm, making this approach suitable for investigating the chemical composition of single cells or even subcellular structures [38]. SIMS is based on irradiation of the sample surface by a primary beam of high energy containing metal ions (e.g. Ar^{+}, Ge^{+}, or In^{+}). These primary ions generate the emission of secondary ions from the sample surface. The energy of the primary ion is much higher (range 5–25 keV) than the energy of the laser beam in MALDI experiments; thus, SIMS often leads to extensive fragmentation of surface molecules and is classified as a hard ionization technique. SIMS typically desorbs and ionizes elements and small molecules, such as lipids, metabolites, and small drugs, with an upper mass limit about 2 kDa. However, ion beams can be focused with a much higher spatial precision than laser beams. SIMS represents a unique tool for high-resolution IMS of single cells, their organelles and structures or to accurately define tissue regions [53]. This technique does not require any special sample preparation or a matrix. SIMS analyses are carried out in an ultrahigh vacuum (<10^{-7} Pa) to facilitate the transfer of ions after desorption from the sample surface.

SIMS is commonly combined with TOF, magnetic sector or Orbitrap analyzers [54]. According to the experimental design, SIMS works in either the static or dynamic mode. In the static mode, a primary ion beam is used at a dose less than 10^{12} primary ions/cm^2 for desorption of the molecule from the surface and provides information about the composition of the surface. Static SIMS is mostly used for qualitative imaging. Dynamic SIMS is more destructive because a much larger primary ion dose ($>10^{12}$ primary ions/cm^2) is applied on the sample, uncovering deep structures. Dynamic SIMS is mainly used for quantitative elemental imaging [55].

DESI MS

The DESI ionization technique was developed by the Cooks group in 2004 [56] and was first used for MS imaging of biological tissues in 2005 [57]. The DESI principle is based on the concept of the combination of two MS ionization methods—electrospray ionization (ESI) and desorption ionization (DI). DESI occurs by the interaction of charged droplets of solvent (often a mixture of water and methanol at a ratio of 1:1) produced by electrospray with the sample surface. By the collisions of drops with the sample surface, secondary charged droplets containing dissolved surface molecules of sample are generated. These secondary droplets are immediately converted on gaseous ions, which are directed at an appropriate angle into the inlet of the mass analyzer [58]. DESI provides several advantages compared with MALDI and SIMS. DESI is performed at atmospheric pressure and requires no additional sample preparation or addition of the organic matrix. DESI also induces very little fragmentation of the sample, making it suitable for analysis of complex molecules. DESI provides multiply charged ions in the form of $[M + nH]^{n+}$ and $[M - nH]^{n-}$ but at a lower spatial resolution than MALDI or SIMS [53]. The rapid analysis time and its ability to be combined with various MS analyzers make this technique attractive for imaging all types of tissue [51] or particular structures, including polymers, drugs, and lipids [59].

Application of MALDI-TOF MS in tissue analysis

MALDI-TOF MS for tissue analysis has already demonstrated its applicability in clinical and biological problems [60-62]. The generation of tissue-specific molecular weight or *m/z* maps or images with high resolution and sensitivity provides a tool for pathology, chemotherapeutics, and discovery of disease biomarkers. MALDI-TOF MS allows the rapid detection of more than a thousand peptides and proteins from various tissues covering diverse fields of medicine, ranging from oncology, regenerative medicine, and neurology to pathology, tissue architecture or biomedical research [42, 45, 62-68]. MALDI MS or IMS, with laser capture microdissection, generates expression profiles from individual cells or clinicopathologically relevant regions of tissue. For example, the molecular profiles of tumor tissues can correctly predict tumor behavior, diagnosis, prognosis or response to therapy. Bottom-up proteomics based on complex patterns can lead to the discovery of novel biomarkers [42, 65].

MALDI-TOF MS/IMS has the potential to identify patient subpopulations that are not evident based on the cellular phenotype determined microscopically [58]. In surgical pathology, IMS allows the highly sensitive and rapid evaluation of surgical intraoperative margins [69]. The IMS spectra generated in high resolution from tumor lesions surrounded by healthy tissue requires sophisticated computational analysis to correctly discriminate and classify the samples. For this purpose, a new method was developed involving reconstructing the image from the raw mass-spectral data, preprocessing of IMS data and subsequent classification and identification of IMS data based on artificial neural networks (ANNs) [70]. ANNs are computational simulations of human neural networks for modeling highly nonlinear systems in which the relationship between the variables is unknown or very complex [71].

Histological staining and IMS

Histological staining remains a cornerstone in the routine diagnosis of cellular and tissue pathomorphology. Classical histological techniques require skilled clinical pathologists to diagnose tissue abnormalities. Spectral profiles or images can complement structural information and facilitate or specify a diagnosis [72]. Correct interpretation of MALDI MS/IMS information requires the correlation of specific ion images to histological information. The latter can be accomplished either using the same tissue section for both MALDI MS/IMS and histopathology or by analysis of two consecutive sections. The first approach is complicated by interference of the dye used for tissue staining with ionization during MS. Covalent binding of a dye—e.g., hematoxylin/eosin (H&E)—to the sample surface, reduces the quality of a mass spectrum. However, chemically distinct dyes, such as cresyl violet or methylene blue, are compatible [72]. Nevertheless, the staining pattern provided by these dyes is different than that provided by H&E, and pathological information does not need to be exhaustive. Recently, a staining protocol for tissue sections already analyzed by MS was introduced that allowed a clear correlation to MALDI IMS results [73]. Analysis of consecutive sections requires a precise alignment of neighboring structures. This is often complicated in complex samples, such as neural tissue samples, due to the different microarchitecture and molecular profiles of adjacent tissue sections [74].

The data outlined above apply only to fresh-frozen tissue samples. As the commonly used stains, including H&E, are compatible with formalin-fixed paraffin-embedded tissues [36], the presence of a cross-linked surface due to formalin bridges introduced by fixation of FFPE tissues prevents analysis by MS. The peptide cross-links can be released using enzymatic treatment to make the surface available for MS analysis [75]. The availability of FFPE samples archived throughout the clinical facilities represents an enormously rich material for detailed MS/IMS studies with clear links to clinical practice [76].

NP-Mediated IMS

Nanoscale materials have been widely introduced into bioanalytical MS and IMS research rather recently to overcome obstacles in MS analysis of complex or unstable biological samples. Although it has been demonstrated that classical organic chemical matrices in MALDI-TOF MS enable the detection of peptides, proteins and nucleic acids and other biomolecules [77], there are still unresolved problems in the adaptation of MALDI-TOF MS protocols to IMS:

1) The co-crystallization of analytes with matrices does not produce homogeneous mixtures, which cause hot spots, thereby requiring sweet-spot searching [78].
2) MALDI-TOF MS can hardly detect small molecules because of the high background signals coming from small organic matrices, which are present in the low-mass region (500 Da) [79].
3) The presence of salts in a sample solution increases the intensities of salt-adducted forms [80].
4) Neutral molecules such as carbohydrates are poorly ionized by MALDI because of the absence of either a basic or an acidic group in their structures [81].

To resolve these problems, the use of inorganic compounds with NP properties as matrices has been introduced for the determination of analytes ranging from small organic molecules to biopolymers [82-85].

MALDI requires photon-absorbing matrix compounds to enhance desorption [86]. UV-absorbing materials can be used as energy mediators to transfer the photon energy from the laser source to the surrounding analytes for effective desorption and ionization with minimum fragmentation of analyte molecules. Cobalt NPs (30 nm in diameter) as matrices have been used by the pioneers in the MALDI field for the analysis of lysozyme [87]. The cobalt NPs possess a large surface area, show high photoabsorption, and a low heat capacity compared with those of microparticles. Inspired by Tanaka's results, a series of inorganic micro- and nanomaterials have been investigated as potential inorganic matrices—e.g., graphite particles [88], AuNPs [89], silver NPs [90, 91], titanium dioxide NPs [82, 92], silicon NPs and nanorods [93, 94], Au nanorods [95], and carbon nanotubes [96].

Nanomaterial matrices compared with organic matrices offer better sample homogeneity [82, 89, 90, 92-99] and elimination of matrix ion interference. Flocculated and trapped mixtures can be detected using nanomaterials in various matrices [100-102]. AuNPs are suitable matrices for the determination of biomolecules in high-salt solutions, such as biological buffers, by MALDI-TOF MS [102]. AuNP-assisted laser desorption/ionization (LDI) was used for the determination of neutral carbohydrates [81], where the ionization efficiency of neutral carbohydrates can be greatly amplified without derivatization steps. Bare, capped, and functionalized AuNPs are good candidates as new generation matrices for high-resolution imaging and profiling analysis [87]. As described elsewhere, AuNPs are particularly interesting because they do not (or seldom) ionize by laser irradiation; however, a local temperature increase occurs on the particle surface [103]. Heat produced by the laser beam is then rapidly transferred to the analyzed sample. As a result, molecules of the analyte are desorbed/ionized with minimal background signal coming from the matrix. Compared with a commonly used 2,5-dihydrobenzoic acid matrix, the AuNPs showed the successful detection of small carbohydrates up to m/z 500 [101].

AuNPs were demonstrated to mediate the ionization of several peptide systems and small proteins [89, 97, 100-102, 104-108]. Additionally, the complexity and size of AuNPs influence the ionization of biomolecules in MALDI experiments. Russell and co-workers [106] published the detection of peptides with molecular weights of 500–2500 using 2- to 10-nm AuNPs. Moreover, coating AuNPs (functionalization) allows for selective extraction of desired substances from the complex solutions [89, 109]. For example, polyethylene-modified magnetic NPs (Fe_3O_4) to extract phosphoproteins from complex protein digests for MS analysis were used (Chen et al. 2011). Interestingly, the deposition method—e.g., the order of the layout of reagents and sample—influences either the interaction of the AuNP matrix with the sample or exposition of the sample to the laser beam. Samples covered with AuNPs provided better detection sensitivity and sample homogeneity compared with either the deposition of a mixture of matrix and sample onto the target plate or deposition of AuNPs onto the target before the sample [110].

NPs is now widely applied in various fields of tissue visualization—e.g., immunohistochemistry [13], MS profiling and imaging [38, 42, 60], detection of individual biomolecules in living cells, delivery as vectors [34, 35, 111] or systemic tracking of defined cell populations in whole organisms [11, 22]. Modification and functionalization of their surface, selection of their physical properties and biological targeting make NPs highly attractive for diagnosis, targeted therapy and biomedical research. A brief overview of the use of NPs in tissue visualization is provided in Fig. 19.8.
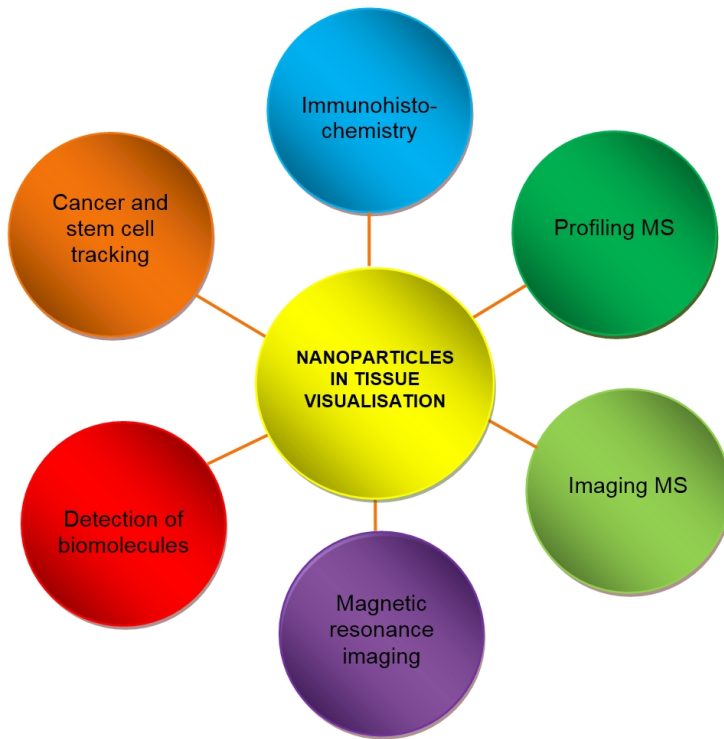
FIGURE 19.8
Brief overview of NP use in tissue visualization

Conclusions

Nanomaterials have wide applications in visualization strategies in cell and tissue biology. In particular, specifically engineered NPs can complement classical techniques of analysis on fixed tissues and enhance the performance of *in vivo* MRI. Biocompatible NPs provide a tool for *in vivo* cell tracking in regenerative medicine or cancer research and provide deep insight into tissue ultrastructure and chemical composition. IMS combines efficient analysis of chemical composition, spatial distribution and structural information, reflecting the complexity of the biological systems. Classical histological staining techniques are still indispensable particularly for daily clinical routine; however, the use of advanced methods such as NP-mediated IMS complement greatly the palette of available diagnostic approaches in the clinic and research.

Bringing the bioanalytical MS analysis to the cellular and subcellular levels allows the identification of molecular composition related to precise spatial localization. The combination of structural visualization and bioanalytical analysis complements greatly and contributes to the entanglement of complex interactions and mechanistic phenomena in tissues. Therefore, nanomaterial-mediated visualization is an important tool in standard clinicopathological techniques and tissue engineering.

Acknowledgements

References

1. Perkin WH. Producing a new coloring matter for dyeing with a lilac or purple color stuffs of silk, cotton, wool, or other matherials. London: British Patent No. 1984. Filed 26th August; 1856.
2. Golgi C. Sulla structtura della sostanza grigiadela ervello. Gazetta Medica Lomberda. 1873;33:244-6.
3. Transidico P, Bianchi M, Capra M, Pelicci PG, Faretta M. From cells to tissues: fluorescence confocal microscopy in the study of histological samples. Microsc Res Tech. 2004 Jun 1;64(2):89-95.
4. Schone C, Hofler H, Walch A. MALDI imaging mass spectrometry in cancer research: combining proteomic profiling and histological evaluation. Clin Biochem. 2013 Apr;46(6):539-45.
5. Yasunaga M, Furuta M, Ogata K, Koga Y, Yamamoto Y, Takigahira M, Matsumura Y. The significance of microscopic mass spectrometry with high resolution in the visualisation of drug distribution. Sci Rep. 2013;3:3050.
6. Roulhac PL, Ward JM, Thompson JW, Soderblom EJ, Silva M, Moseley MA, 3rd, Jarvis ED. Microproteomics: quantitative proteomic profiling of small numbers of laser-captured cells. Cold Spring Harb Protoc. 2011;2011(2):pdb prot5573.
7. IHC World 2013. Available from: http://www.ihcworld.com/index.htm.
8. Auffan M, Rose J, Bottero JY, Lowry GV, Jolivet JP, Wiesner MR. Towards a definition of inorganic nanoparticles from an environmental, health and safety perspective. Nat Nanotechnol. 2009 Oct;4(10):634-41.
9. Karathanasis E, Chan L, Balusu SR, D'Orsi CJ, Annapragada AV, Sechopoulos I, Bellamkonda RV. Multifunctional nanocarriers for mammographic quantification of tumor dosing and prognosis of breast cancer therapy. Biomaterials. 2008 Dec;29(36):4815-22.
10. Gao X, Yang L, Petros Ja, Marshall FF, Simons JW, Nie S. In vivo molecular and cellular imaging with quantum dots. Current opinion in biotechnology. 2005;16(1):63-72.
11. Michalet X, Pinaud FF, Bentolila LA, Tsay JM, Doose S, Li JJ, Sundaresan G, Wu AM, Gambhir SS, Weiss S. Quantum dots for live cells, in vivo imaging, and diagnostics. Science (New York, N.Y.). 2005;307(5709):538-44.
12. Hachani R, Lowdell M, Birchall M, Thanh NT. Tracking stem cells in tissue-engineered organs using magnetic nanoparticles. Nanoscale. 2013 Oct 9.

13. Fan K, Cao C, Pan Y, Lu D, Yang D, Feng J, Song L, Liang M, Yan X. Magnetoferritin nanoparticles for targeting and visualizing tumour tissues. Nat Nanotechnol. 2012 Jul;7(7):459-64.

14. Wu TJ, Tzeng YK, Chang WW, Cheng CA, Kuo Y, Chien CH, Chang HC, Yu J. Tracking the engraftment and regenerative capabilities of transplanted lung stem cells using fluorescent nanodiamonds. Nat Nanotechnol. 2013;8(9):682-9.

15. Tietz O, Kamaly N, Smith G, Shamsaei E, Bhakoo KK, Long NJ, Aboagye EO. Design, synthesis and in vitro characterization of fluorescent and paramagnetic CXCR4-targeted imaging agents. American Journal of Nuclear Medicine and Molecular Imaging. 2013;3(4):372-83.

16. Sykova E, Jendelova P. Magnetic resonance tracking of implanted adult and embryonic stem cells in injured brain and spinal cord. Annals of the New York Academy of Sciences. 2005 May;1049:146-60.

17. Reimer P, Balzer T. Ferucarbotran (Resovist): a new clinically approved RES-specific contrast agent for contrast-enhanced MRI of the liver: properties, clinical development, and applications. European Radiology. 2003 Jun;13(6):1266-76.

18. Richmond H, Zwerner J, Kim Y, Fiorentino D. Nephrogenic systemic fibrosis: relationship to gadolinium and response to photopheresis. Archives of Dermatology. 2007 Aug;143(8):1025-30.

19. He L, Feng L, Cheng L, Liu Y, Li Z, Peng R, Li Y, Guo L, Liu Z. Multilayer Dual-Polymer-Coated Upconversion Nanoparticles for Multimodal Imaging and Serum-Enhanced Gene Delivery. ACS Applied Materials & Interfaces. 2013;5(20):10381-8.

20. Mehravi B, Ahmadi M, Amanlou M, Mostaar A, Ardestani MS, Ghalandarlaki N. Conjugation of glucosamine with Gd(3+)-based nanoporous silica using a heterobifunctional ANB-NOS crosslinker for imaging of cancer cells. International Journal of Nanomedicine. 2013;8:3383-94.

21. Rowe MD, Thamm DH, Kraft SL, Boyes SG. Polymer-modified gadolinium metal-organic framework nanoparticles used as multifunctional nanomedicines for the targeted imaging and treatment of cancer. Biomacromolecules. 2009 Apr 13;10(4):983-93.

22. Lien Z-Y, Hsu T-C, Liu K-K, Liao W-S, Hwang K-C, Chao J-I. Cancer cell labeling and tracking using fluorescent and magnetic nanodiamond. Biomaterials. 2012;33(26):6172-85.

23. Hammerstingl R, Huppertz A, Breuer J, Balzer T, Blakeborough A, Carter R, Fuste LC, Heinz-Peer G, Judmaier W, Laniado M, Manfredi RM, Mathieu DG, Muller D, Mortele K, Reimer P, Reiser MF, Robinson PJ, Shamsi K, Strotzer M, Taupitz M, Tombach B, Valeri G, van Beers BE, Vogl TJ. Diagnostic efficacy of gadoxetic acid (Primovist)-enhanced MRI and spiral CT for a therapeutic strategy: comparison with intraoperative and histopathologic findings in focal liver lesions. European Radiology. 2008 Mar;18(3):457-67.

24. Morlieras J, Chezal JM, Miot-Noirault E, Roux A, Heinrich-Balard L, Cohen R, Tarrit S, Truillet C, Mignot A, Hachani R, Kryza D, Antoine R, Dugourd P, Perriat P, Janier M, Sancey L, Lux F, Tillement O. Development of gadolinium based nanoparticles having an affinity towards melanin. Nanoscale. 2013 Feb 21;5(4):1603-15.

25. England CG, Priest T, Zhang G, Sun X, Patel DN, McNally LR, van Berkel V, Gobin AM, Frieboes HB. Enhanced penetration into 3D cell culture using two and three layered gold nanoparticles. International Journal of Nanomedicine. 2013;8:3603-17.

26. Deerinck TJ, Giepmans BNG, Smarr BL, Martone ME, Ellisman MH. Light and electron microscopic localization of multiple proteins using quantum dots. Methods Mol Biol. 2007;374:43-53.

27. Maltez-da Costa M, de la Escosura-Muñiz A, Nogués C, Barrios L, Ibáñez E, Merkoçi A. Simple monitoring of cancer cells using nanoparticles. Nano letters. 2012;12(8):4164-71.

28. Kim T, Momin E, Choi J, Yuan K, Zaidi H, Kim J, Park M, Lee N, McMahon MT, Quinones-Hinojosa A, Bulte JW, Hyeon T, Gilad AA. Mesoporous silica-coated hollow manganese oxide nanoparticles as positive T1 contrast agents for labeling and MRI tracking of adipose-derived mesenchymal stem cells. Journal of the American Chemical Society. 2011 Mar 9;133(9):2955-61.

29. Huxford RC, Della Rocca J, Lin W. Metal-organic frameworks as potential drug carriers. Current opinion in chemical biology. 2010;14(2):262-8.

30. Rieter WJ, Taylor KML, An H, Lin W, Lin W. Nanoscale metal-organic frameworks as potential multimodal contrast enhancing agents. Journal of the American Chemical Society. 2006;128(28):9024-5.

31. Taylor KML, Rieter WJ, Lin W. Manganese-based nanoscale metal-organic frameworks for magnetic resonance imaging. Journal of the American Chemical Society. 2008;130(44):14358-9.

32. Foucault-Collet A, Gogick KA, White KA, Villette S, Pallier A, Collet G, Kieda C, Li T, Geib SJ, Rosi NL, Petoud S. Lanthanide near infrared imaging in living cells with Yb3+ nano metal organic frameworks. Proceedings of the National Academy of Sciences of the United States of America. 2013 Oct 22;110(43):17199-204.

33. Della Rocca J, Liu D, Lin W. Nanoscale metal-organic frameworks for biomedical imaging and drug delivery. Accounts of chemical research. 2011;44(10):957-68.

34. Prigodich AE, Seferos DS, Massich MD, Giljohann DA, Lane BC, Mirkin CA. Nano-flares for mRNA regulation and detection. ACS Nano. 2009 Aug 25;3(8):2147-52.

35. Seferos DS, Giljohann DA, Hill HD, Prigodich AE, Mirkin CA. Nano-flares: probes for transfection and mRNA detection in living cells. Journal of the American Chemical Society. 2007 Dec 19;129(50):15477-9.

36. Seeley EH, Caprioli RM. MALDI imaging mass spectrometry of human tissue: method challenges and clinical perspectives. Trends in biotechnology. 2011;29(3):136-43.

37. Seeley EH, Schwamborn K, Caprioli RM. Imaging of intact tissue sections: moving beyond the microscope. Journal of Biological Chemistry. 2011;286(29):25459-66.

38. Lanni EJ, Rubakhin SS, Sweedler JV. Mass spectrometry imaging and profiling of single cells. Journal of proteomics. 2012;75(16):5036-51.

39. Oppenheimer SR, Drexler DM. Tissue analysis by imaging MS. Bioanalysis. 2012;4(1):95-112.

40. Chaurand P, Norris JL, Cornett DS, Mobley JA, Caprioli RM. New developments in profiling and imaging of proteins from tissue sections by MALDI mass spectrometry. Journal of proteome research. 2006 Nov;5(11):2889-900.

41. Casadonte R, Caprioli RM. Proteomic analysis of formalin-fixed paraffin-embedded tissue by MALDI imaging mass spectrometry. Nature Protocols. 2011 Nov;6(11):1695-709.

42. Caldwell RL, Caprioli RM. Tissue profiling by mass spectrometry: a review of methodology and applications. Molecular & Cellular Proteomics. 2005;4(4):394-401.

43. Fuchsberger C, Hübl H, Schäfer G, Pelzer A, Bartsch G, Klocker H, Barbarini N, Bellazzi R, Wieder W, Bonn G. Analysis and Visualization of Spatial Proteomic Data for Tissue Characterization. 2008 21st IEEE International Symposium on Computer-Based Medical Systems. 2008;8(5):185-90.

44. Kaletaş BK, van der Wiel IM, Stauber J, Güzel C, Kros JM, Luider TM, Heeren RMa. Sample preparation issues for tissue imaging by imaging MS. Proteomics. 2009;9(10):2622-33.

45. Reyzer ML, Caprioli RM. MALDI mass spectrometry for direct tissue analysis: a new tool for biomarker discovery. Journal of proteome research. 2005;4(4):1138-42.

46. Karas M, Hillenkamp F. Laser desorption ionization of proteins with molecular masses exceeding 10,000 daltons. Analytical Chemistry. 1988;60(20):2299-301.

47. Vickerman JC. Molecular imaging and depth profiling by mass spectrometry--SIMS, MALDI or DESI? The Analyst. 2011;136(11):2199-217.

48. Liu J, Ouyang Z. Mass spectrometry imaging for biomedical applications. Analytical and bioanalytical chemistry. 2013;405(17):5645-53.

49. Schwartz SA, Reyzer ML, Caprioli RM. Direct tissue analysis using matrix-assisted laser desorption/ionization mass spectrometry: practical aspects of sample preparation. Journal of Mass Spectrometry. 2003 Jul;38(7):699-708.

50. Mounfield WP, 3rd, Garrett TJ. Automated MALDI matrix coating system for multiple tissue samples for imaging mass spectrometry. Journal of the American Society for Mass Spectrometry. 2012 Mar;23(3):563-9.

51. Weaver EM, Hummon AB. Imaging mass spectrometry: from tissue sections to cell cultures. Advanced Drug Delivery Reviews. 2013;65(8):1039-55.

52. Castaing R, Slodzian G. Microanalyse par emission ionique secondaire. Journal of Microscopie. 1962;1:395-410.

53. Chughtai K, Heeren RMA. Mass spectrometric imaging for biomedical tissue analysis. Chemical Reviews. 2010;110(5):3237-77.

54. Boxer SG, Kraft ML, Weber PK. Advances in imaging secondary ion mass spectrometry for biological samples. Annual review of biophysics. 2009;38:53-74.

55. Amstalden van Hove ER, Smith DF, Heeren RMa. A concise review of mass spectrometry imaging. Journal of chromatography. A. 2010;1217(25):3946-54.

56. Takáts Z, Wiseman JM, Gologan B, Cooks RG. Mass spectrometry sampling under ambient conditions with desorption electrospray ionization. Science (New York, N.Y.). 2004;306(5695):471-3.

57. Wiseman JM, Puolitaival SM, Takáts Z, Cooks RG, Caprioli RM. Mass spectrometric profiling of intact biological tissue by using desorption electrospray ionization. Angewandte Chemie (International ed. in English). 2005;44(43):7094-7.

58. Cooks RG, Ouyang Z, Takats Z, Wiseman JM. Detection Technologies. Ambient mass spectrometry. Science (New York, N.Y.). 2006;311(5767):1566-70.

59. Vismeh R, Waldon DJ, Teffera Y, Zhao Z. Localization and quantification of drugs in animal tissues by use of desorption electrospray ionization mass spectrometry imaging. Analytical Chemistry. 2012;84(12):5439-45.

60. Agar NYR, Malcolm JG, Mohan V, Yang HW, Johnson MD, Tannenbaum A, Agar JN, Black PM. Imaging of meningioma progression by matrix-assisted laser desorption ionization time-of-flight mass spectrometry. Analytical Chemistry. 2010;82(7):2621-5.

61. Agar NYR, Yang HW, Carroll RS, Black PM, Agar JN. Matrix solution fixation: histology-compatible tissue preparation for MALDI mass spectrometry imaging. Analytical Chemistry. 2007;79(19):7416-23.

62. Caldwell RL, Opalenik SR, Davidson JM, Caprioli RM, Nanney LB. Tissue profiling MALDI mass spectrometry reveals prominent calcium-binding proteins in the proteome of regenerative MRL mouse wounds. Wound Repair and Regeneration. 2008;16(3):442-9.

63. Feng X, Liu X, Luo Q, Liu B-f. Mass spectrometry in systems biology: an overview. Mass spectrometry reviews. 2008;27(6):635-60.

64. Liu X, Wen F, Yang J, Chen L, Wei Y-q. A review of current applications of mass spectrometry for neuroproteomics in epilepsy. Mass spectrometry reviews. 2010;29(2):197-246.

65. Nanney LB, Caldwell RL, Pollins AC, Cardwell NL, Opalenik SR, Davidson JM. Novel Approaches for Understanding the Mechanisms of Wound Repair. Journal of Investigative Dermatology Symposium Proceedings. 2006;11(1):132-9.

66. Narasimhan K, Changqing Z, Choolani M. Ovarian cancer proteomics: Many technologies one goal. Proteomics. Clinical applications. 2008;2(2):195-218.

67. Pan S, Aebersold R, Chen R, Rush J, Goodlett DR, McIntosh MW, Zhang J, Brentnall TA. Mass spectrometry based targeted protein quantification: methods and applications. Journal of proteome research. 2009;8(2):787-97.

68. Zhang X, Wei D, Yap Y, Li L, Guo S, Chen F. Mass spectrometry-based "omics" technologies in cancer diagnostics. Mass spectrometry reviews. 2007;26(3):403-31.

69. Kang S, Kim MJ, An H, Kim BG, Choi YP, Kang KS, Gao MQ, Park H, Na HJ, Kim HK, Yun HR, Kim DS, Cho NH. Proteomic molecular portrait of interface zone in breast cancer. Journal of proteome research. 2010 Nov 5;9(11):5638-45.

70. Xiong X-C, Fang X, Ou Y-Z, Jiang Y, Huang Z-J, Zhang Y-K. Artificial Neural Networks for Classification and Identification of Data of Biological Tissue Obtained by Mass-Spectrometry Imaging. Chinese Journal of Analytical Chemistry. 2012;40(1):43-9.

71. Amato F, López A, Peña-Méndez EM, Vaňhara P, Hampl A, Havel J. Artificial neural networks in medical diagnosis. Journal of Applied Biomedicine. 2013;11(2):47-58.

72. Chaurand P, Schwartz Sa, Billheimer D, Xu BJ, Crecelius A, Caprioli RM. Integrating histology and imaging mass spectrometry. Analytical Chemistry. 2004;76(4):1145-55.

73. Schwamborn K, Krieg RC, Reska M, Jakse G, Knuechel R, Wellmann A. Identifying prostate carcinoma by MALDI-Imaging. International journal of molecular medicine. 2007;20(2):155-9.

74. Walch A, Rauser S, Deininger S-O, Höfler H. MALDI imaging mass spectrometry for direct tissue analysis: a new frontier for molecular histology. Histochemistry and cell biology. 2008;130(3):421-34.

75. Stauber J, MacAleese L, Franck J, Claude E, Snel M, Kaletas BK, Wiel IM, Wisztorski M, Fournier I, Heeren RM. On-tissue protein identification and imaging by MALDI-ion mobility mass spectrometry. Journal of the American Society for Mass Spectrometry. 2010 Mar;21(3):338-47.

76. Franck J, Arafah K, Elayed M, Bonnel D, Vergara D, Jacquet A, Vinatier D, Wisztorski M, Day R, Fournier I, Salzet M. MALDI imaging mass spectrometry: state of the art technology in clinical proteomics. Molecular & Cellular Proteomics. 2009;8(9):2023-33.

77. Pan C, Xu S, Zhou H, Fu Y, Ye M, Zou H. Recent developments in methods and technology for analysis of biological samples by MALDI-TOF-MS. Analytical and bioanalytical chemistry. 2007;387(1):193-204.

78. Tholey A, Heinzle E. Ionic (liquid) matrices for matrix-assisted laser desorption/ionization mass spectrometry-applications and perspectives. Analytical and bioanalytical chemistry. 2006;386(1):24-37.

79. Guo Z, Zhang Q, Zou H, Guo B, Ni J. A method for the analysis of low-mass molecules by MALDI-TOF mass spectrometry. Analytical Chemistry. 2002;74(7):1637-41.

80. Börnsen KO. Influence of salts, buffers, detergents, solvents, and matrices on MALDI-MS protein analysis in complex mixtures. Methods Mol Biol. 2000;146:387-404.

81. Scalf J, West P. Part I : Introduction to Nanoparticle Characterization with AFM. Santa Clara: Pacific Nanotechnology; 2006. 1-8 p.

82. Castro AL, Madeira PJA, Nunes MR, Costa FM, Florêncio MH. Titanium dioxide anatase as matrix for matrix-assisted laser desorption/ionization analysis of small molecules. Rapid Communications in Mass Spectrometry. 2008;22(23):3761-6.

83. Shan Z, Han L, Yuan M, Deng C, Zhao D, Tu B, Yang P. Mesoporous tungsten titanate as matrix for matrix-assisted laser desorption/ionization time-of-flight mass spectrometry analysis of biomolecules. Analytica chimica acta. 2007;593(1):13-9.

84. Shenar N, Martinez J, Enjalbal C. Laser desorption/ionization mass spectrometry on porous silica and alumina for peptide mass fingerprinting. Journal of the American Society for Mass Spectrometry. 2008;19(5):632-44.

85. Zhang H, Hoogenboom R, Meier MaR, Schubert US. Combinatorial and high-throughput approaches in polymer science. Measurement Science and Technology. 2005;16(1):203-11.

86. Karas M, Krüger R. Ion formation in MALDI: the cluster ionization mechanism. Chemical Reviews. 2003;103(2):427-40.

87. Tanaka K, Ido Y, Akita S, Yoshida Y, Yoshida T, editors. Detection of high mass molecules by laser desorption time-of-flight mass spectrometry1987 1987; Osaka.

88. Zhang H, Cha S, Yeung ES. Colloidal graphite-assisted laser desorption/ionization MS and MS(n) of small molecules. 2. Direct profiling and MS imaging of small metabolites from fruits. Analytical Chemistry. 2007;79(17):6575-84.

89. Duan J, Linman MJ, Chen C-Y, Cheng QJ. CHCA-modified Au nanoparticles for laser desorption ionization mass spectrometric analysis of peptides. Journal of the American Society for Mass Spectrometry. 2009;20(8):1530-9.

90. Chiu T-C, Chang L-C, Chiang C-K, Chang H-T. Determining estrogens using surface-assisted laser desorption/ionization mass spectrometry with silver nanoparticles as the matrix. Journal of the American Society for Mass Spectrometry. 2008;19(9):1343-6.

91. Shrivas K, Wu H-f. Applications of silver nanoparticles capped with different functional groups as the matrix and affinity probes in surface-assisted laser desorption/ionization time-of-flight and atmospheric pressure matrix-assisted laser desorption/ionization ion trap mas. Rapid Communications in Mass Spectrometry. 2008;22(18):2863-72.

92. Chen C-T, Chen Y-C. Fe3O4/TiO2 core/shell nanoparticles as affinity probes for the analysis of phosphopeptides using TiO2 surface-assisted laser desorption/ionization mass spectrometry. Analytical Chemistry. 2005;77(18):5912-9.

93. Piret G, Drobecq H, Coffinier Y, Melnyk O, Boukherroub R. Matrix-free laser desorption/ionization mass spectrometry on silicon nanowire arrays prepared by chemical etching of crystalline silicon. Langmuir : the ACS journal of surfaces and colloids. 2010;26(2):1354-61.

94. Wen X, Dagan S, Wysocki VH. Small-molecule analysis with silicon-nanoparticle-assisted laser desorption/ionization mass spectrometry. Analytical Chemistry. 2007;79(2):434-44.

95. Chen LC, Yonehama J, Ueda T, Hori H, Hiraoka K. Visible-laser desorption/ionization on gold nanostructures. Journal of Mass Spectrometry. 2007;42(3):346-53.

96. Gholipour Y, Nonami H, Erra-Balsells R. In situ analysis of plant tissue underivatized carbohydrates and on-probe enzymatic degraded starch by matrix-assisted laser desorption/ionization time-of-flight mass spectrometry by using carbon nanotubes as matrix. Analytical biochemistry. 2008;383(2):159-67.

97. Huang Y-F, Chang H-T. Analysis of adenosine triphosphate and glutathione through gold nanoparticles assisted laser desorption/ionization mass spectrometry. Analytical Chemistry. 2007;79(13):4852-9.

98. Peterson DS. Matrix-free methods for laser desorption/ionization mass spectrometry. Mass spectrometry reviews. 2007;26(1):19-34.

99. Seino T, Sato H, Yamamoto A, Nemoto A, Torimura M, Tao H. Matrix-free laser desorption/ionization-mass spectrometry using self-assembled germanium nanodots. Analytical Chemistry. 2007;79(13):4827-32.

100. Huang Y-f, Chang H-t. Nile Red-adsorbed gold nanoparticle matrixes for determining aminothiols through surface-assisted laser desorption/ionization mass spectrometry. Analytical Chemistry. 2006;78(5):1485-93.

101. Su C-l, Tseng W-l. Gold nanoparticles as assisted matrix for determining neutral small carbohydrates through laser desorption/ionization time-of-flight mass spectrometry. Analytical Chemistry. 2007;79(4):1626-33.

102. Wu H-P, Yu C-J, Lin C-Y, Lin Y-H, Tseng W-L. Gold nanoparticles as assisted matrices for the detection of biomolecules in a high-salt solution through laser desorption/ionization mass spectrometry. Journal of the American Society for Mass Spectrometry. 2009;20(5):875-82.

103. Schürenberg M, Dreisewerd K, Hillenkamp F. Laser desorption/ionization mass spectrometry of peptides and proteins with particle suspension matrixes. Analytical Chemistry. 1999;71(1):221-9.

104. Altelaar aFM, Klinkert I, Jalink K, de Lange RPJ, Adan RaH, Heeren RMa, Piersma SR. Gold-enhanced biomolecular surface imaging of cells and tissue by SIMS and MALDI mass spectrometry. Analytical Chemistry. 2006;78(3):734-42.

105. Lin P-C, Tseng M-C, Su A-K, Chen Y-J, Lin C-C. Functionalized magnetic nanoparticles for small-molecule isolation, identification, and quantification. Analytical Chemistry. 2007;79(9):3401-8.

106. McLean Ja, Stumpo Ka, Russell DH. Size-selected (2-10 nm) gold nanoparticles for matrix assisted laser desorption ionization of peptides. Journal of the American Chemical Society. 2005;127(15):5304-5.

107. Pujals S, Bastús NG, Pereiro E, López-Iglesias C, Puntes VF, Kogan MJ, Giralt E. Shuttling gold nanoparticles into tumoral cells with an amphipathic proline-rich peptide. Chembiochem : a European journal of chemical biology. 2009;10(6):1025-31.

108. Teng C-H, Ho K-C, Lin Y-S, Chen Y-C. Gold nanoparticles as selective and concentrating probes for samples in MALDI MS analysis. Analytical Chemistry. 2004;76(15):4337-42.

109. Vanderpuije BNY, Han G, Rotello VM, Vachet RW. Mixed monolayer-protected gold nanoclusters as selective peptide extraction agents for MALDI-MS analysis. Analytical Chemistry. 2006;78(15):5491-6.

110. Wu H-P, Su C-L, Chang H-C, Tseng W-L. Sample-first preparation: a method for surface-assisted laser desorption/ionization time-of-flight mass spectrometry analysis of cyclic oligosaccharides. Analytical Chemistry. 2007;79(16):6215-21.

111. Prigodich AE, Randeria PS, Briley WE, Kim NJ, Daniel WL, Giljohann DA, Mirkin CA. Multiplexed nanoflares: mRNA detection in live cells. Analytical Chemistry. 2012 Feb 21;84(4):2062-6.